

¹School of Industrial Technology, Universiti Sains Malaysia, Pulau Pinang, Malaysia

²Department of Civil and Environmental Engineering, Washington State University, Pullman, WA

Introduction

The tropical coasts, a location exposed to all-year intense solar radiation, contribute greatly to the energy, moisture, and carbon exchanges between the air and sea where the mechanism and location responsible for enhanced interactions are critical in improving the global carbon and water budget estimates. This work reports and analyzes eddy covariance and meteorological data collected during the Northeast Monsoon from November 2015 to January 2016.

Site and Instruments

An eddy covariance (EC) station was installed at the edge of the pier of the Centre for Marine & Coastal Studies (CEMACS), Universiti Sains Malaysia in Muka Head shown in Figure 1. The instrumented platform is located at the coast of a Malaysian Forest Reserve designated area (5°28'6"N, 100°12'1"E).

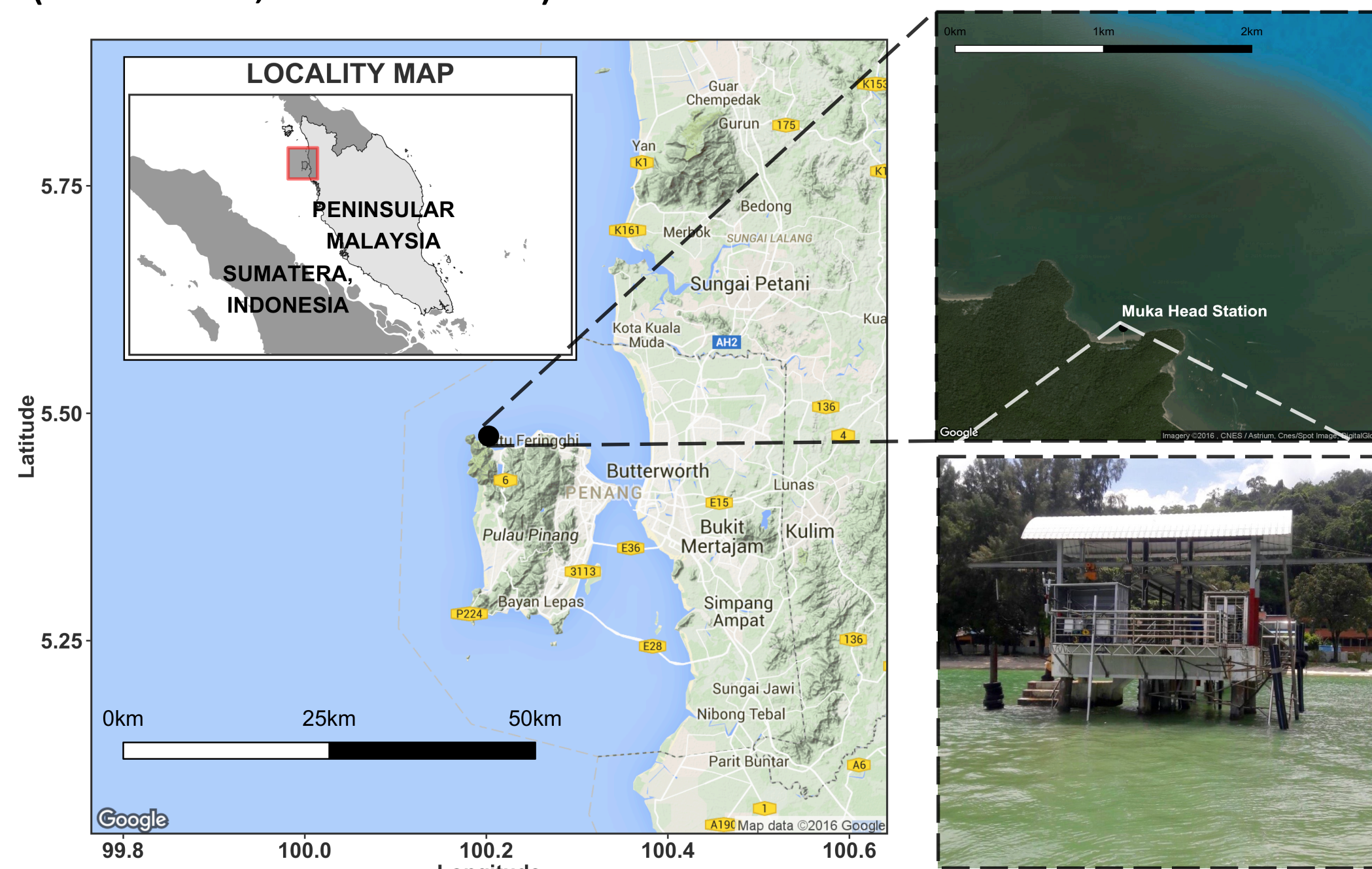


Figure 1. Location of eddy covariance station.

Table 1. List of instruments and measured variables

Instruments	Measured Variables
Open path CO ₂ /H ₂ O gas analyzer (LICOR, LI-7500A) at 4 m	CO ₂ and water vapor flux
Ultrasonic anemometer (YOUNG, 81000) at 4 m	Three-component wind velocities (u, v, w)
Two temperature thermistors (LICOR) at depths of 0.5 m and 2.5 m	Sea surface and beneath the sea surface temperatures
Temperature and relative humidity sensor (HMP155, Vaisala)	Temperature and relative humidity
Pyranometer (LICOR, LI-200SL)	Global radiation
Net radiometer (NR LITE 2, Kipp & Zonen)	Net radiation



Figure 2. CO₂/H₂O gas analyzer and sonic anemometer

Energy Balance Closure

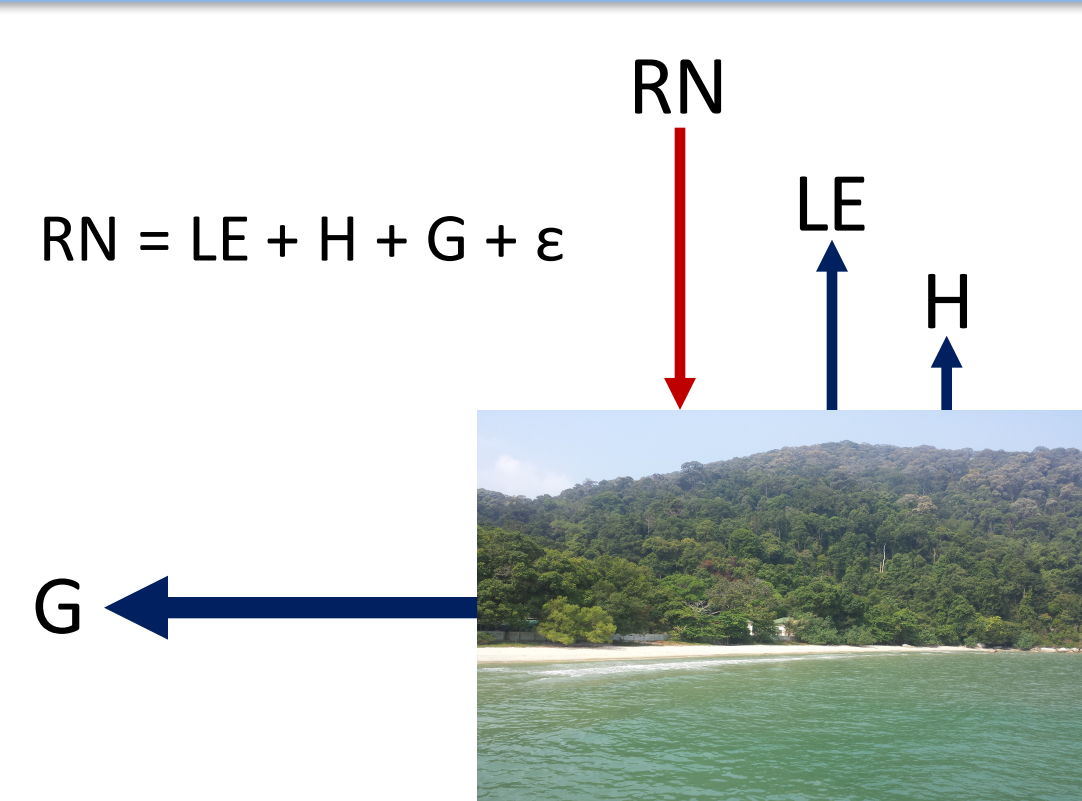


Figure 3. Energy balance at the tropical coast system

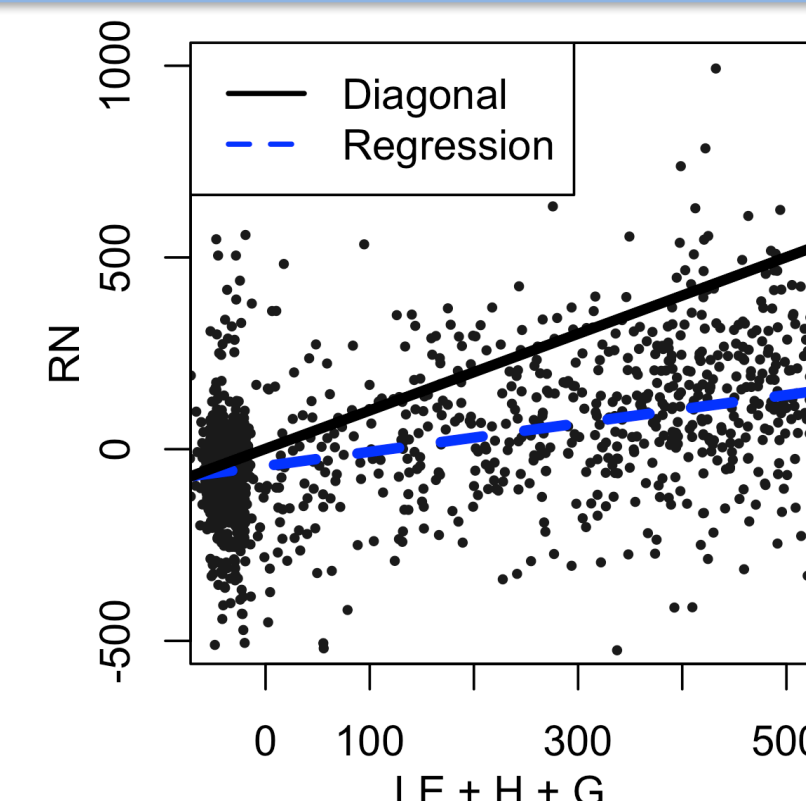


Figure 4. Energy balance at this system; regression line has an R²=0.24

Results

Meteorology

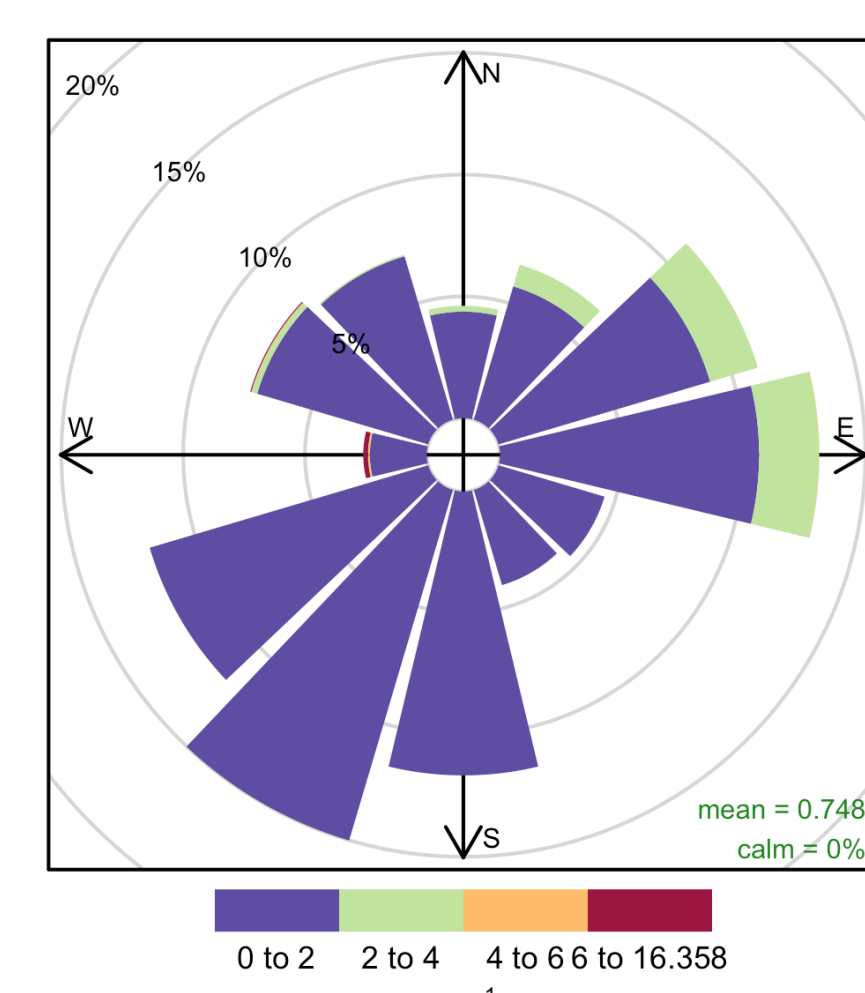


Figure 5. Wind rose for the period Nov 2015 to Apr 2016

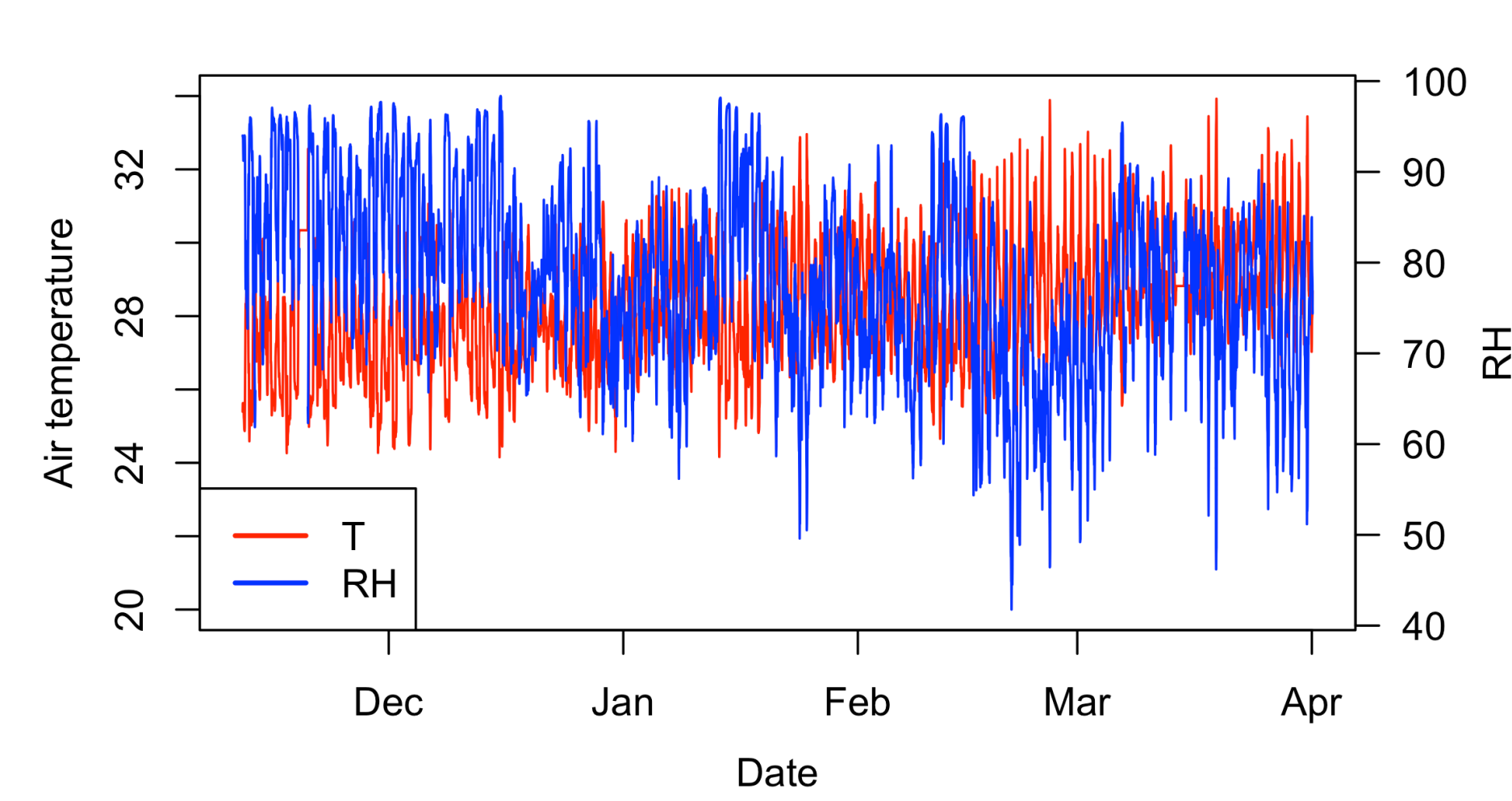


Figure 6. Air temperature (T, °C) and relative humidity (RH, %) in 2015-2016

Latent Heat (LE)

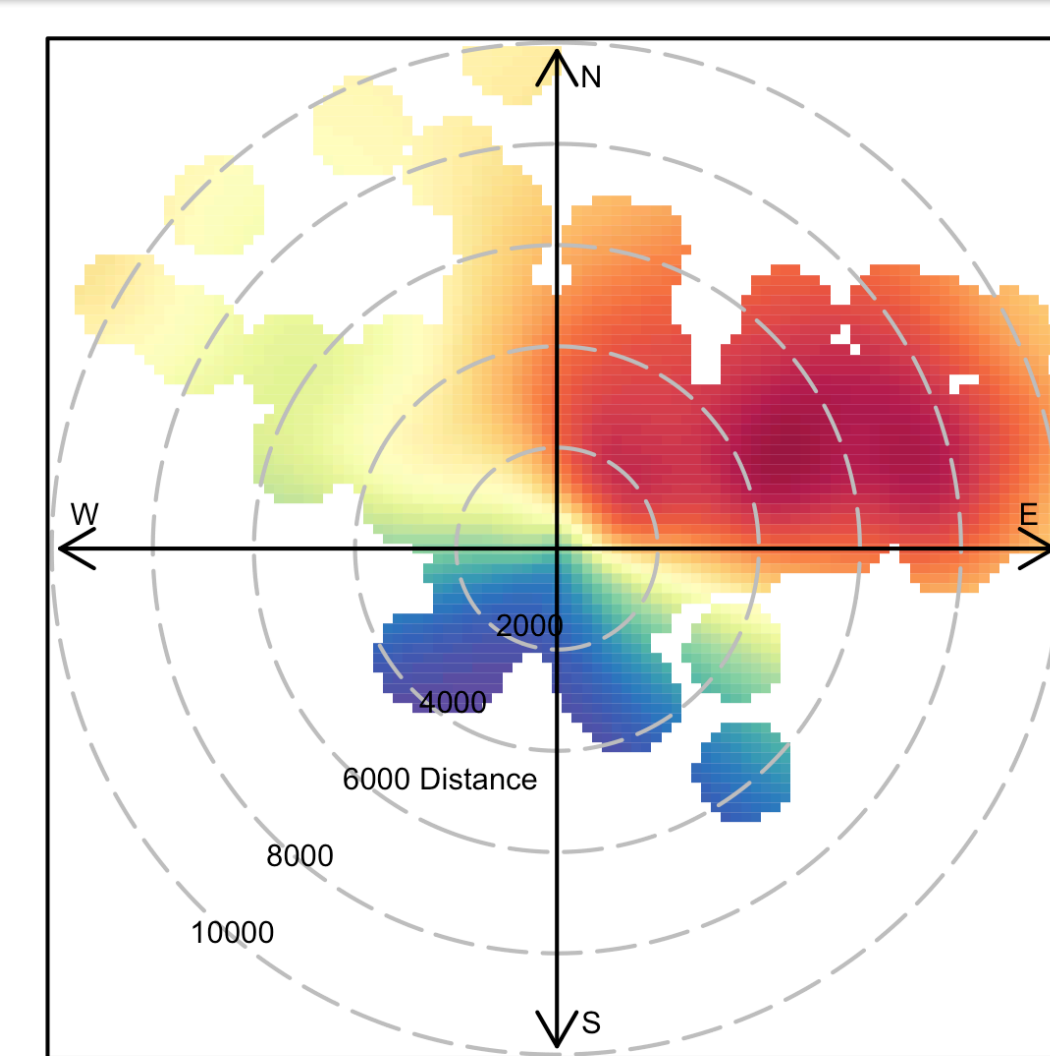


Figure 7. Distance (m) of 90% flux contribution with LE (W m⁻²), values are forced positive for smoothing

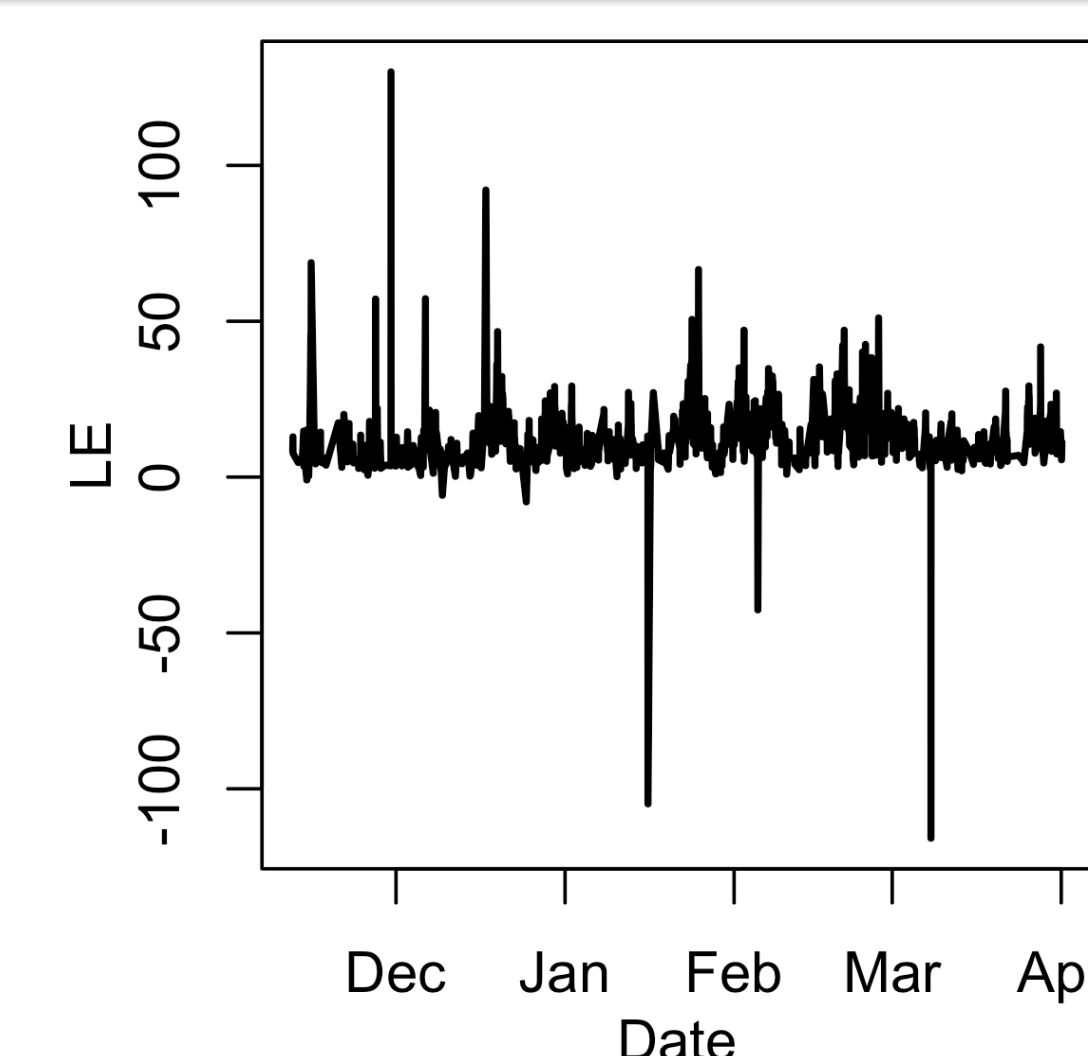


Figure 8. LE (W m⁻²) trend from Nov 2015 to Apr 2016 for wind directions between 0° and 90° and quality check (EddyPro) of 0 or 1

Sensible Heat (H)

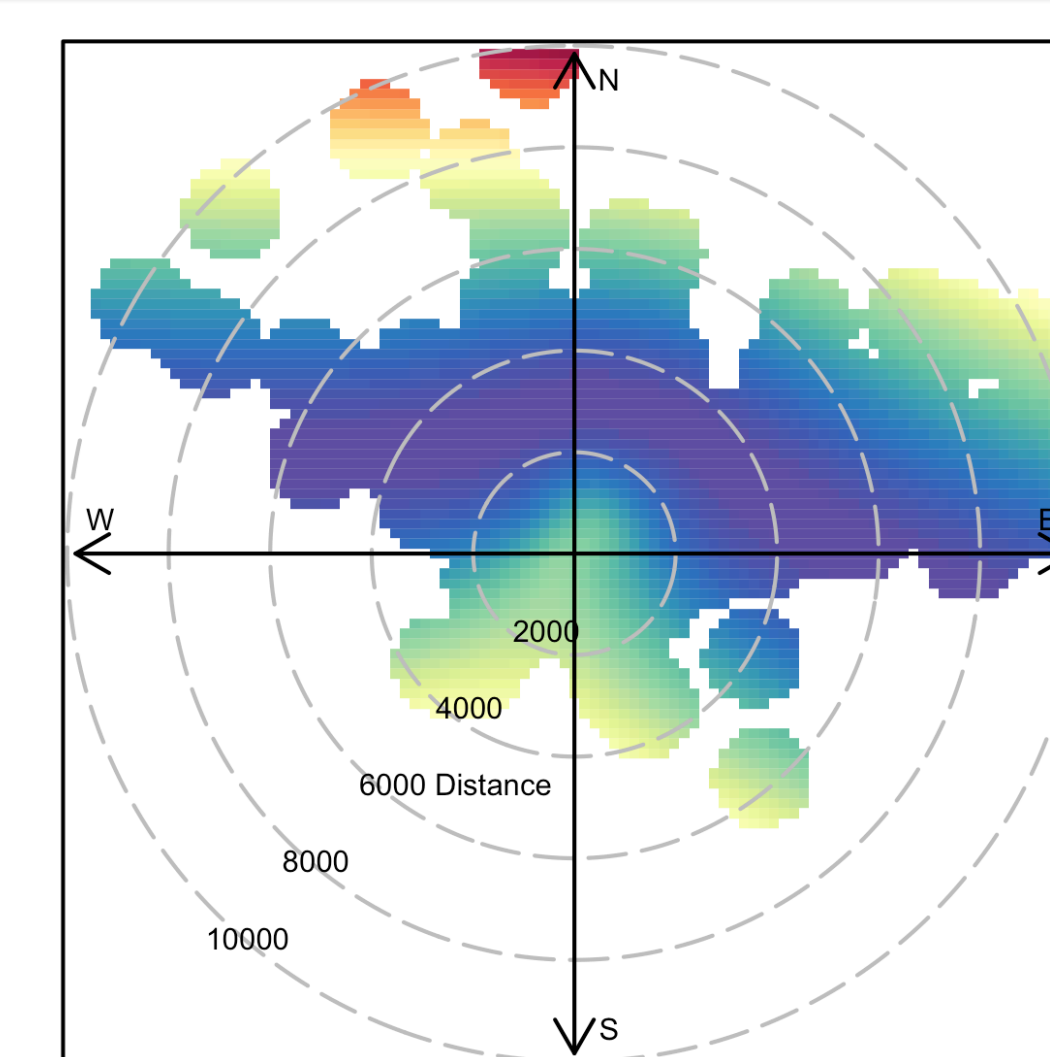


Figure 9. Distance (m) of 90% flux contribution with H (W m⁻²), values are forced positive for smoothing

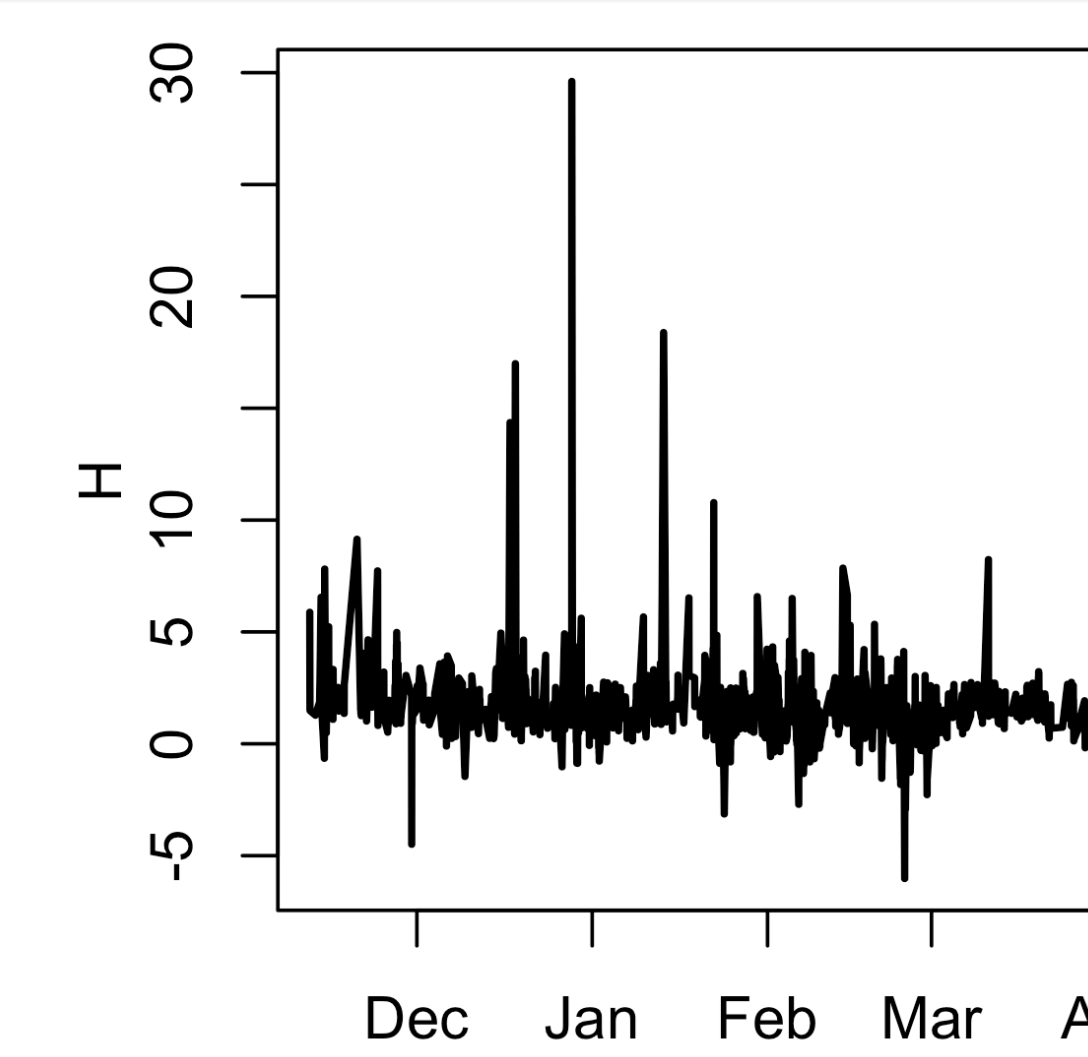


Figure 10. H (W m⁻²) trend from Nov 2015 to Apr 2016 for wind directions between 0° and 90° and quality check (EddyPro) of 0 or 1

CO₂ Flux

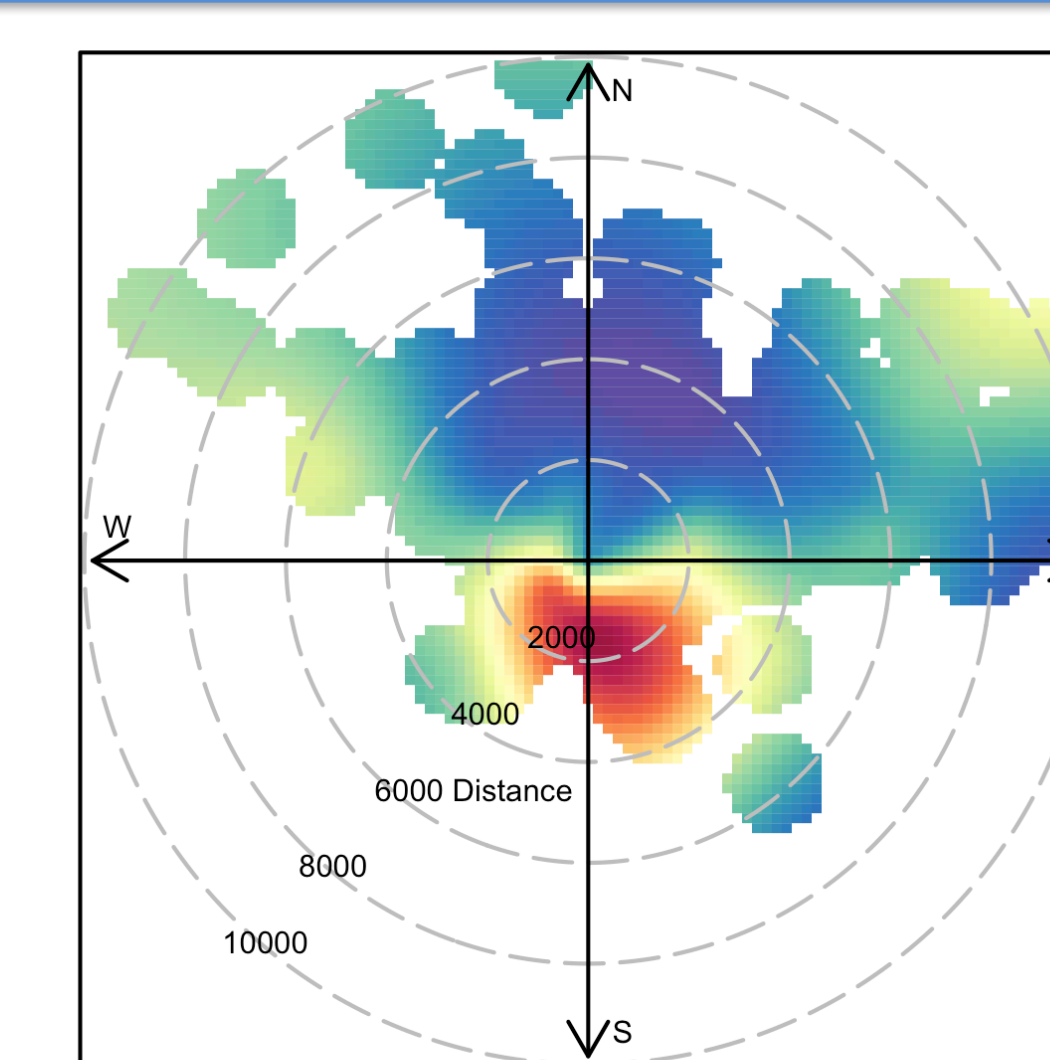


Figure 11. Distance (m) of 90% flux contribution with CO₂ (μmol m⁻² s⁻¹), values are forced positive for smoothing

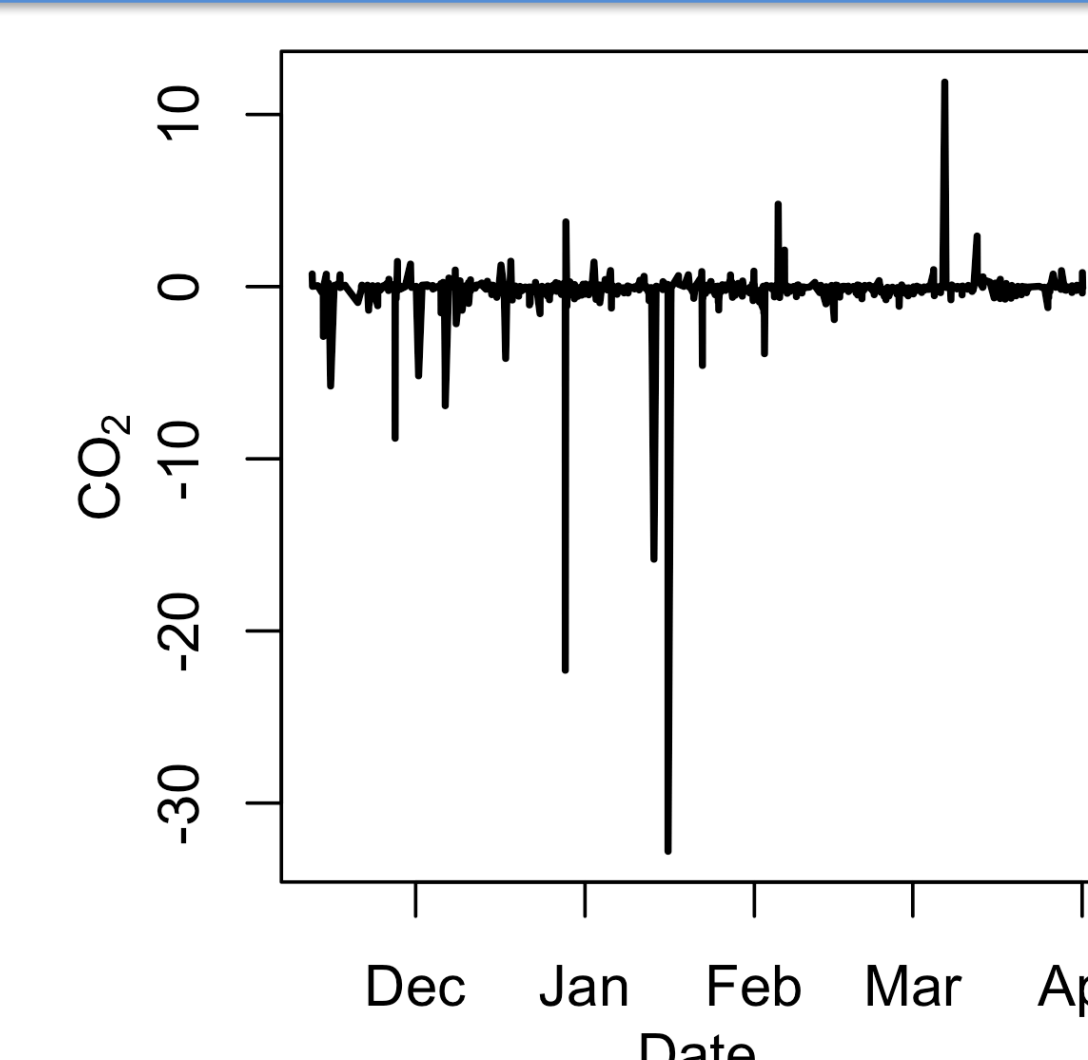


Figure 12. CO₂ (μmol m⁻² s⁻¹) trend from Nov 2015 to Apr 2016 for wind directions between 0° and 90° and quality check (EddyPro) of 0 or 1

Discussion

- About 50% of flux data is not usable due to direction of wind from land but only for wind speeds <1 m/s. Most high wind speed conditions and 90% flux contribution originated from the Northeast, which is the sea. (Figure 5)
- Sensible and latent heat fluxes were relatively low, which ranged from -5 - 30 W m⁻² and -100 - 200 W m⁻² respectively with the highest latent and sensible heat fluxes occurring at 16:00 LT (Figures 8 and 10). This is possibly due to weak winds.
- Analysis of CO₂ fluxes revealed that this coastal tropical ocean is a weak carbon sink, which ranged from -1.2 - -0.2 μmol m⁻² s⁻¹, with the maximum sink occurring concurrently with the highest latent and sensible heat fluxes.
- Diurnal meteorological trends showed that mean global radiation peaked at 800 W m⁻² in the afternoon while mean net radiation only reached a maximum of 700 W m⁻² possibly due to reflected radiation and heavy clouds; both occurred at approximately 14:00 LT. (Figure 14)
- Two underwater temperature sensors at 0.5 m and 1.5 m beneath the water surface showed that the temperatures varied greatly and caused high energy storage in the water, 28 - 33°C, with the coolest and hottest temperature occurring at 08:00 LT and 16:00 LT, respectively. (Figure 15)
- Calculated heat stored by the water showed the tropical coast system released energy at a mean of -2000 W m⁻² during the night and absorbed heat at a mean of 1200 W m⁻² during the day with a maximum release of heat at 16:00 LT. (Figure 16)

Surface Energy Budget

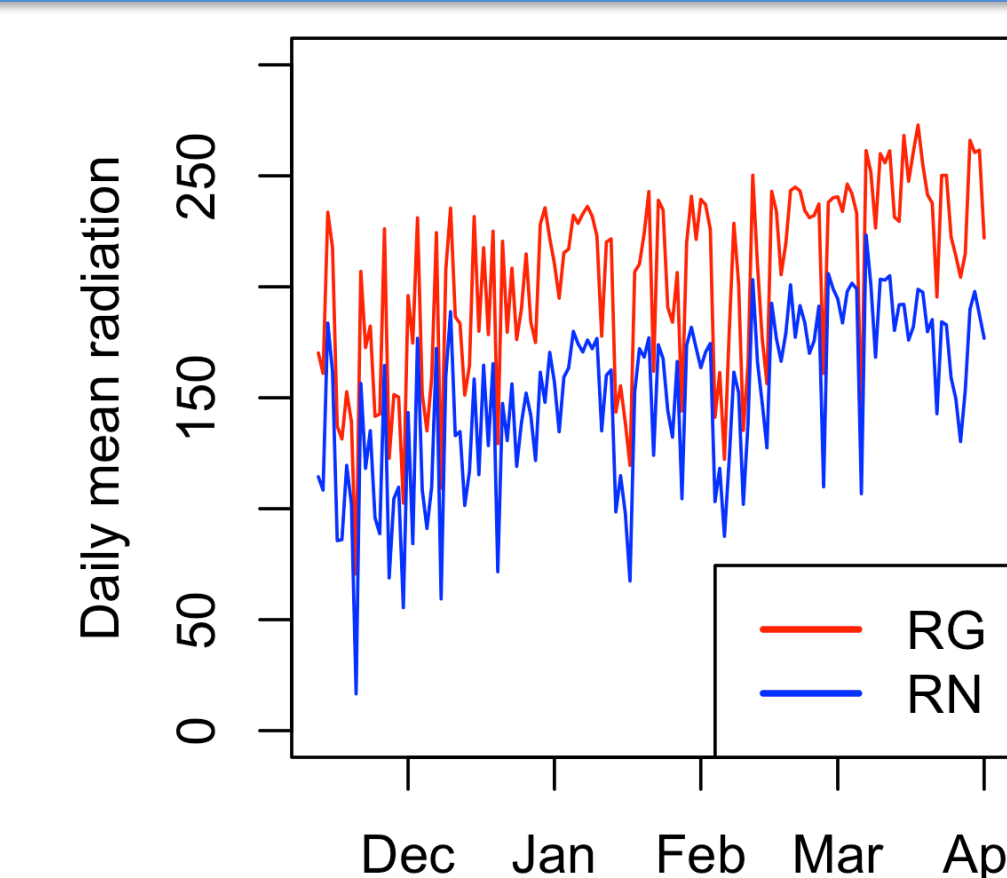


Figure 13. Daily averaged global (RG) and net (RN) radiation in 2015-2016

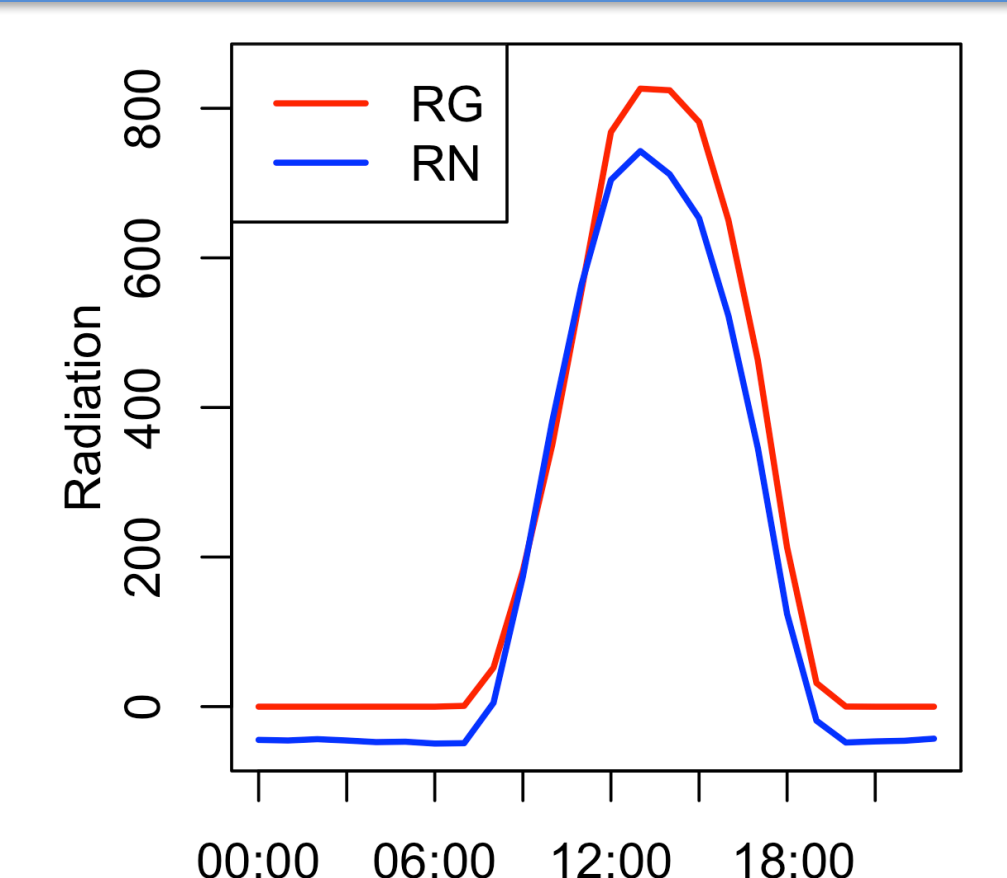


Figure 14. Diurnally averaged global (RG) and net (RN) radiation in 2015-2016

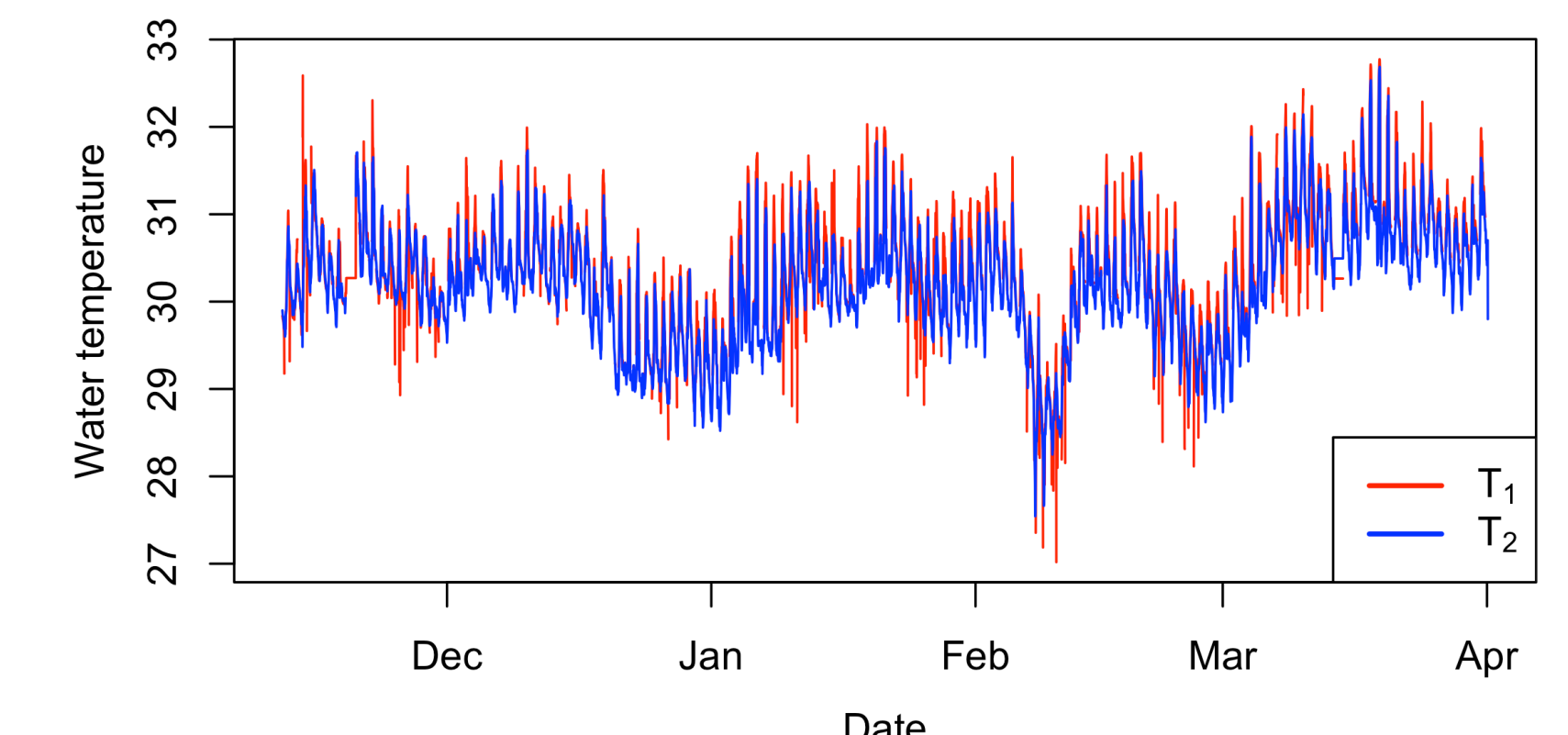


Figure 15. Underwater temperatures (°C) trends at two levels in 2015-2016; T₁ is near the surface while T₂ is deeper underwater near to the seabed; the difference in height between the two sensors is 1 m

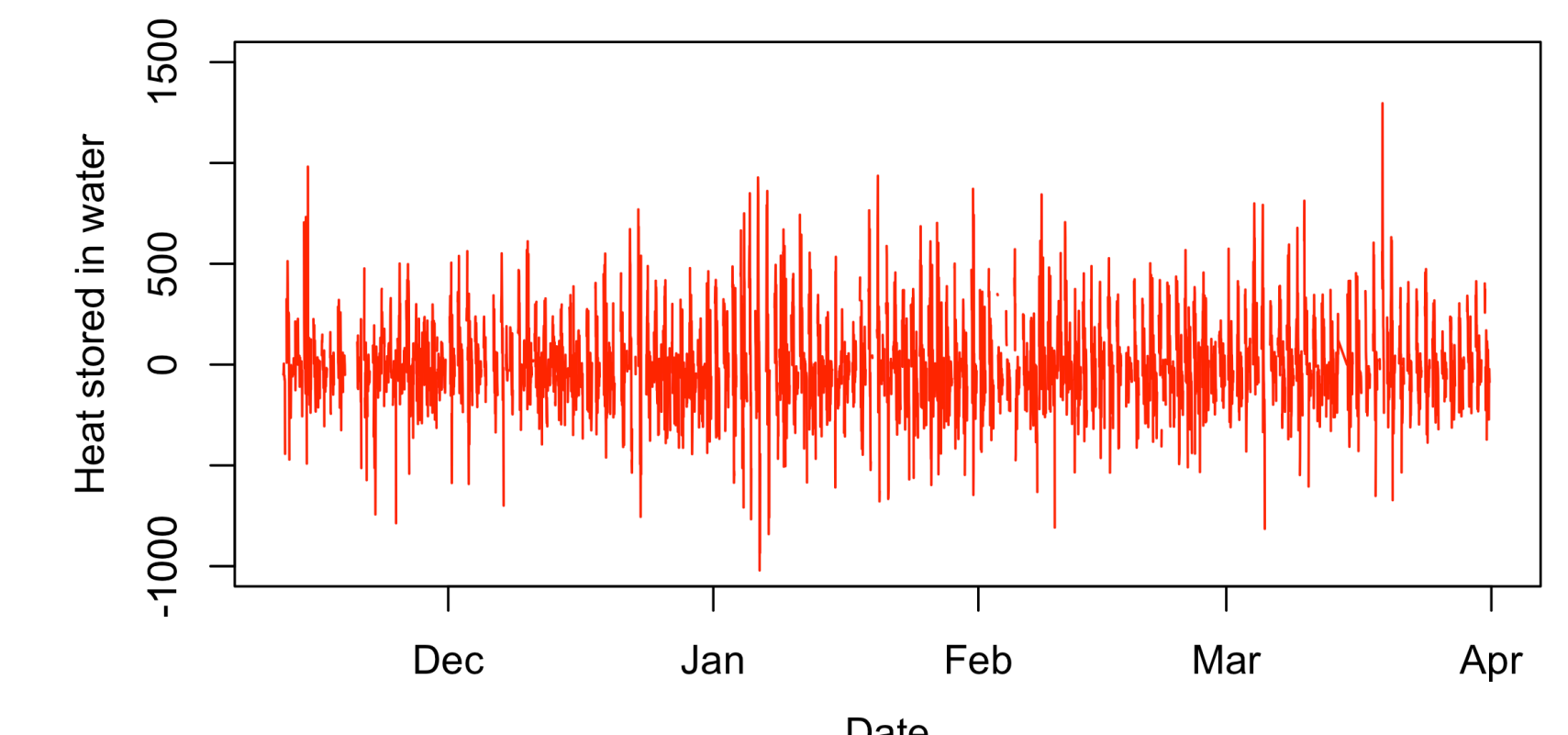


Figure 16. Heat stored (G) in water (W m⁻²) trend in 2015-2016.

Conclusions

- Global and net radiation increased from November 2015 to April 2016, which consequently increased air temperature.
- Primary energy flow into and out of the tropical coast system is heat stored in water.
- Latent and sensible heats and CO₂ flux were low due to weak winds.